Classical and Advanced Computational Plate/Shell Models for Piezoelectric Laminated Structures

E. Carrera, S. Brischetto & M. Cinefra
Aerospace Department, Politecnico di Torino, Italy

ABSTRACT: This lectures is devoted to advanced computational models for multilayered plate/shell structures embedding piezoelectric layers as sensor/actuators. The hierarchical modelling is obtained by referring to the Carrera Unified Formulation which permits the development of equivalent single-layer and layer-wise theories based on classical and mixed variational statements. The need of layer-wise analysis is pointed out as well as the convenience to refer to mixed variational statements to evaluate transverse mechanical and electrical variables without any post-processing. Mostly an overview of the recent work co-authored by the first author is given. The results have been obtained by running an in-house software recently named *MUL2.*

1 *INTRODUCTION*

Smart systems are the candidate for next generation structures of aerospace vehicles as well as for some advanced products of automotive and ship industries. Piezoelectric materials are the most used in that framework. These materials are characterized by the so called 'direct' and 'inverse effect': an applied electrical potential induces mechanical stresses and vice-versa. Such an electro-mechanical coupling permits one to build up closed-loop control systems in which piezo-materials play the role of both actuators and sensors. An intelligent structure can be therefore built in which, for instance, deformations or vibrations are reduced by appropriate control laws [1].

In many of the recent applications, piezoelectric layers are employed in conjunction with composites layered structures. A smart structure is in this case obtained by embedding piezo-layers (sensors and/or actuators) in a multilayered one. Among the various open problems of smart structures such as material capabilities, optimum design, control algorithm, this work is direct to modelling of plate/shell structures. Accurate evaluation of electrical and mechanical variables is, in fact, a crucial point for appropriate use smart structures. It is a well known, see [2], [3], [4], that classical theories, that were originally developed for traditional plates and shells for pure mechanical-problems, can lead to large errors when applied to multilayered cases embedding piezolayers. This is mainly due to the following features: 1. layers exhibit different electro-mechanical material properties which make feasible quasi three-dimensional mechanical/electrical fields; 2. a strong coupling can occur between mechanical and electrical fields; 3. piezoelectric materials are often introduced as localized patches.

An efficient description of the above three points require amendments to those plate/shell theories that were originally introduced for pure mechanical problems and structures made by isotropic materials. No effective control, in fact, can be build unless accurate evaluation of electrical (voltage, electric field, charge) and mechanical (displacement,

stress, strain) variables is made. Smart structures specialists know that available commercial general-purpose FE codes do not offer efficient shell elements on that respect.

This lectures is devoted to discuss the methods and ideas that permit to 'fight' against points 1-3. The following points are covered.

- Evaluation of electromechanical coupling stiffness.
- Discussion of higher order theories.
- Application of Zig-Zag (ZZ) theories with Interlaminar Continuous (IC) electrical and mechanical fields.
- Layer-wise description of mechanical and electrical layers.
- Variable kinematic approach based on Carrera Unified Formulation (CUF).
- Mixed methods applied to piezoelectricity along with direct evaluation of secondary electro-mechanical variables such as electric displacement and charge. Attention is restricted to Reissner Mixed Variational Theorem (RMVT).
- Efficiency of the 2D model in sensing and actuating.

All the above problems are discussed by both analytical and computational (FE) method as well as for plate and shell geometries.

The contribution brought by authors and co-workers are considered at the most in the lecture with minor reference to some other relevant works made in the last ten years literature. Among the author's papers the recent papers [5]-[10] are referred to.

2 *2D MODELS VS AND C_z^0-REQUIREMENTS*

Laminated piezoelectric structures are characterized by piece-wise constant distribution of mechanical properties in the thickness plate/shell direction. As a consequence in-plane stresses are in general discontinuous at the each layer interface. On the other hand, due to equilibrium conditions, transverse shear and normal stresses must be continuous at the interfaces. The continuity of the normal stresses requires that strains must be discontinuous since material properties change from layer to layer; as a consequence the derivatives of the displacements must be discontinuous at each interface (ZZ effect). The normal electric displacement must be continuous at the interface too, if free boundary conditions are postulated. The set of this rules has been summarized in [11] as C_z^0-requirements: mechanical and electrical displacements as well as transverse stresses (not their derivatives) must be C^0 continuous functions in the z-thickness direction. An example of stresses, displacements and electric displacements is shown in Fig.1. The fulfillment of C_z^0–requirements consists of a key-point in the development of advanced theories for the analysis of piezoelectric plate/shell structures.

If classical formulations based on extension to piezoelectricity of Principle of Virtual Displacements (PVD) are employed transverse normal and shear stresses as well as transverse electrical displacement are 'a posteriori' obtained discontinuous at the interface. Such an error could be reduced by increasing the accuracy of 2D theories as well as by adopting refined layer-wise theories.

Better results are obtained by employing extended Reissner Mixed Variational Theorem (RMVT) to piezoelectricity. RMVT permits, in fact, to assume 'a priori' transverse

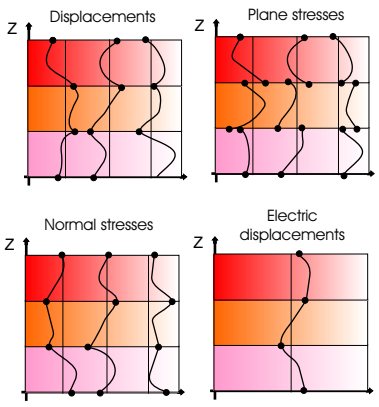

Figure 1: Example of displacements, stresses and electric displacements distribution along the in z-coordinate.

shear/normal stresses and/or transverse electrical displacement as continuous function in the thickness direction.

It appears clear from the discussion above that the following possibilities arise to build refined and advanced model for piezoelectric laminated structures:

1. to increase the order of the expansion of the unknown variables in the thickness plate/shell direction.
2. to use both ESL and LW description for the unknown variables;
3. to refer to mixed variational statement to get 'a priori' continuity of a given electro-mechanical variable.

These three points are discussed and adopted in this work. The complexity inside Points 1 and 2 are handled by means of Unified Formulation (CUF) introduced by Carrera in [12]. Point 3 is considered by employing various forms of original Reissner Mixed variational Theorem.

3 *THE CARRERA UNIFIED FORMULATION*

The unified formulation consists of a technique which permits to handle in a unified manner a large variety of plate modelings. This is made by expressing governing equations and/or finite element matrices in term of a few fundamental 3×3 nuclei which do not formally depend on: - expansion N used to in the z-direction; - number of the node N_n of the element; - variables description (LW or ESL).

3.0.1 *FORMULATION BASED ON PVD*

Unknown variables are in this case the displacements and the electrical potential. The following 'axiomatic' expansion is used for displacements:

$$\boldsymbol{u}^{k}(x,y,z) = F_b(z)\boldsymbol{u}_b^{k}(x,y) + F_r(z)\boldsymbol{u}_r^{k}(x,y) + F_t(z)\boldsymbol{u}_t^{k}(x,y) \qquad r = 2,\ldots,N-1 \tag{1}$$

or in compact form:

$$\boldsymbol{u}^{k}(x,y,z) = F_\tau\, \boldsymbol{u}_\tau^{k} \tag{2}$$

$F_\tau(z)$ are function of the thickness coordinate z which can assume different forms. $\mathbf{u}_\tau$ are two-dimensional 2D unknowns. Similarly, the electric potential is assumed:

$$\phi^k(x,y,z) = F_b(z)\phi_b^k(x,y) + F_r(z)\phi_r^k(x,y) + F_t(z)\phi_t^k(x,y) \qquad r = 2,\ldots,N-1 \quad (3)$$

or un compact form:

$$\phi^k(x,y,z) = F_\tau\, \phi_\tau^k \quad (4)$$

Thickness functions could be the same of those already used for displacements. Of course this is not mandatory and in same cases it could be not convenient.

3.0.2 *FORMULATION BASED ON RMVT*

The transverse normal stresses should be added as field variables in the RMVT applications with respect to those already introduced for the PVD case. The transverse normal stresses are:

$$\boldsymbol{\sigma}_n^k(x,y,z) = F_b(z)\boldsymbol{\sigma}_{nb}^k(x,y) + F_r(z)\boldsymbol{\sigma}_{nr}^k(x,y) + F_t(z)\boldsymbol{\sigma}_{nt}^k(x,y) \qquad r = 2,\ldots,N-1 \quad (5)$$

or in compact form:

$$\boldsymbol{\sigma}_n^k(x,y,z) = F_\tau\, \boldsymbol{\sigma}_{n\tau}^k \quad (6)$$

Also in this case the thickness functions can be the same of those already used for displacements and electric potential. See next sub-sections.

3.1 *EQUIVALENT SINGLE LAYER MODELS*

The assumption above can be used at layer or at multilayer level: LW and ESL theories are than obtained, respectively. Depending on the made choice for the polynomials $F(z)$ a large variety of plate modelings can be introduced. In the ESL case the laminate is treated as a single layer. The subscript k, is therefore omitted.

A first natural choice for thickness functions $F(z)$) consist to refer to power of z polynomials:

$$F_b = 1, \quad F_r = z^{(r-1)}, \quad F_t = z^N \quad r = 2,\ldots,N \quad (7)$$

That is a Taylor-type expansion and the variables related to F_b corresponds to the middle plane values; higher order terms correspond instead to higher order derivative calculated with correspondence to the reference surface of the plate.

To be noticed that this model is not able to reproduce the Zig-Zag form for the displacement field in the thickness direction. Murakami [13] introduced a Zig-Zag function, able to describe a zig-zag form for the displacements. The Murakami Zig-Zag function can be, for instance, introduced instead of the F_t polynomial:

$$F_b = 1, \quad F_t = (-1)^k\zeta_k, \quad F_r = z^{(r-1)} \quad r = 2,\ldots,N. \quad (8)$$

The exponent k changes the sign of the zig-zag term in each layer. Such an artifice permits one to reproduce the discontinuity of the first derivative of the displacements in the z-direction.

The displacements are the only unknowns that could be modelled by ESL model with the introduction of Murakami's zig-zag function. The electrical potential as well as transverse stresses require layer-wise description.

3.2 *LAYER WISE MODELS LW*

If detailed response of individual layers is required and if significant variations in gradients between layers exist, Layer Wise model must be referred to. Each layer is seen as an independent layer and the continuity of the field variables at the interfaces is imposed as a constraint. The use of Taylor type expansion in each layer is not convenient. Top-bottom continuity would require additional conditions on the field variables. In order to avoid this drawback an appropriate combination of Legendre Polynomials could be conveniently used as base function according to the following:

$$F_t = \frac{P_0 + P_1}{2}, \quad F_b = \frac{P_0 - P_1}{2}, \quad F_r = P_r - P_{r-2} \quad r = 2, \ldots, N \tag{9}$$

Where $P_i(\zeta_k)$ is the i-order Legendre polynomial in the domain $-1 \leq \zeta_k \leq 1$. The first five Legendre polynomials are:

$$P_0 = 1 \qquad P_1 = \zeta_k \qquad P_2 = \frac{3\zeta^2 - 1}{2} \qquad P_3 = \frac{5\zeta^3 - 3\zeta}{2} \qquad P_4 = \frac{35\zeta^4 - 30\zeta^2 + 3}{8} \tag{10}$$

The functions we have chosen have the following properties:

$$\zeta_k = \begin{cases} 1: & F_t = 1, \quad F_b = 0, \quad F_r = 0 \\ -1: & F_t = 0, \quad F_b = 1, \quad F_r = 0 \end{cases} \tag{11}$$

For instance, if displacement variables $\boldsymbol{u}_t^k$ e $\boldsymbol{u}_b^k$ are the top and bottom displacement of the k^{th} layer, the continuity condition is easily written as:

$$\boldsymbol{u}_t^k = \boldsymbol{u}_b^{(k+1)}, \quad \text{con} \quad k = 1, \ldots, N_L - 1 \tag{12}$$

Electric potential and transverse stresses are in this work always described as LW variables.

3.3 *ACRONYMS*

Depending on the used variational statement (PVD or RMVT), variables description and order of expansion N a number of two-dimensional theories and related FEs can be derived. In order to identify the various FEs appropriate acronyms are introduced. Fig.(2) shows how the acronyms are built.The first field can be 'E' or 'L' according to ESL or LW description, respectively; the second field can be 'D' or 'M' according to PVD or RMVT application, respectively; the last field can assume the numbers 1-4 according to the order of the adopted expansion in the thickness direction; a third 'Z' and fourth 'C' field (which are optional in the ESL case), denote the use of MZZF and/or IC fulfillment, respectively.

4 *VARIATIONAL STATEMENTS*

Variational statements are used to derive weak and strong form governing equations in the theory of structures. Classical formulations based on extended virtual work principle (Principle of Virtual Displacements, PVD) do not lead to direct evaluation of electrical charge Q. PVD, in fact, states

$$\text{P}VD(u, \phi) : \int_V \left(\delta \boldsymbol{\epsilon}_{pG}^T \boldsymbol{\sigma}_{pC} + \delta \boldsymbol{\epsilon}_{nG}^T \boldsymbol{\sigma}_{nC} - \delta \boldsymbol{\mathcal{E}}_{pG}^T \boldsymbol{\mathcal{D}}_{pC} - \delta \boldsymbol{\mathcal{E}}_{nG}^T \boldsymbol{\mathcal{D}}_{nC} \right) dV = \delta L_e - \delta L_{in}, \tag{13}$$

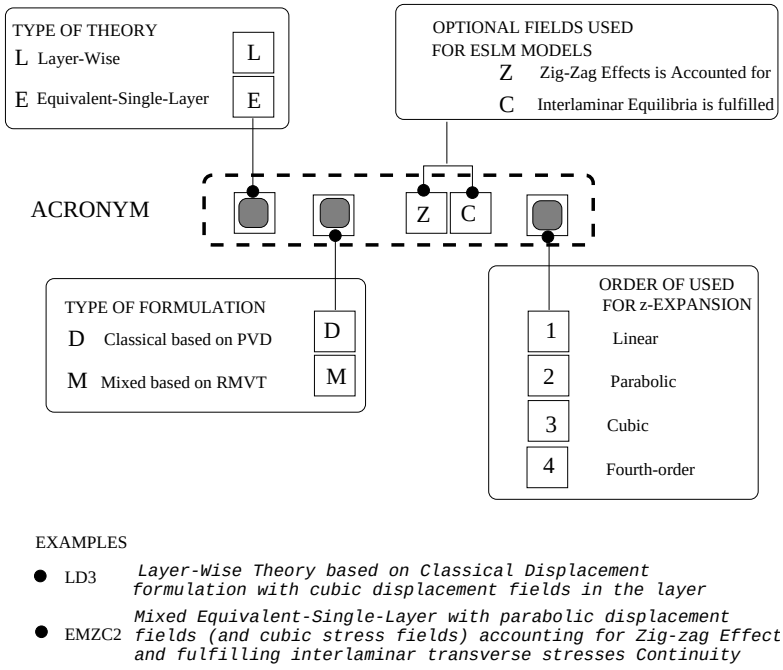

Figure 2: Meanings of the introduced Acronyms.

in which δ is the variational symbol and bold letters denote arrays; strains $\boldsymbol{\epsilon}$ and stresses $\boldsymbol{\sigma}$ have been split into in-plane shell/plate components (subscript p) and transverse ones (subscript n); the same is done for the electrical field $\boldsymbol{\mathcal{E}}$ and electrical displacements $\boldsymbol{\mathcal{D}}$; subscript C and G denote variables from constitutive equations and geometrical relations, respectively. L_e and L_{in} denote external and inertia work, respectively; V is the body volume; T denotes transposition of arrays.

Mechanical displacements and electric potential are the assumed variables. Appropriate post-processing is, therefore, necessary to compute additional variables such as strains, stresses, electrical fields, electrical displacement and electrical charge.

A particular case of PVD which neglects electrical stiffness is:

$$\mathrm{P}VD(u) : \int_V \left(\delta\boldsymbol{\epsilon}_{pG}^T\boldsymbol{\sigma}_{pC} + \delta\boldsymbol{\epsilon}_{nG}^T\boldsymbol{\sigma}_{nC}\right)dV = \delta L_e - \delta L_{in} + \delta L_{elett} \tag{14}$$

where δL_{elett} is the external work done for electric potential.

PVD is used in conjunction to the generalized geometrical relations between displacement (mechanical/electrical components) and strains (mechanical/electrical components), which in general case of shell are written:

$$\boldsymbol{\epsilon}_{pG} = \left[\epsilon_{\alpha\alpha}, \epsilon_{\beta\beta}, \epsilon_{\alpha\beta}\right]^T = \left(\boldsymbol{D}_p + \boldsymbol{A}_p\right)\boldsymbol{u}\ ,\ \boldsymbol{\epsilon}_{nG} = \left[\epsilon_{\alpha z}, \epsilon_{\beta z}, \epsilon_{zz}\right]^T = \left(\boldsymbol{D}_{n\Omega} + \boldsymbol{D}_{nz} - \boldsymbol{A}_n\right)\boldsymbol{u}$$
$$\boldsymbol{\mathcal{E}}_{pG} = \left[\mathcal{E}_\alpha, \mathcal{E}_\beta\right]^T = -\boldsymbol{D}_{e\Omega}\,\boldsymbol{\Phi}\ ,\ \boldsymbol{\mathcal{E}}_{nG} = \left[\mathcal{E}_z\right]^T = -\boldsymbol{D}_{en}\,\boldsymbol{\Phi} \tag{15}$$

where (α, β, z) is the shell reference system (see Fig.4). The explicit form of the introduced arrays follows:

$$\boldsymbol{D}_p = \begin{bmatrix} \frac{\partial_\alpha}{H_\alpha} & 0 & 0 \\ 0 & \frac{\partial_\beta}{H_\beta} & 0 \\ \frac{\partial_\beta}{H_\beta} & \frac{\partial_\alpha}{H_\alpha} & 0 \end{bmatrix} \quad \boldsymbol{D}_{n\Omega} = \begin{bmatrix} 0 & 0 & \frac{\partial_\alpha}{H_\alpha} \\ 0 & 0 & \frac{\partial_\beta}{H_\beta} \\ 0 & 0 & 0 \end{bmatrix} \quad \boldsymbol{D}_{nz} = \begin{bmatrix} \partial_z & 0 & 0 \\ 0 & \partial_z & 0 \\ 0 & 0 & \partial_z \end{bmatrix} \tag{16}$$

$$\boldsymbol{D}_{e\Omega}=\begin{bmatrix}\frac{\partial_\alpha}{H_\alpha} & 0 & 0\\ 0 & \frac{\partial_\beta}{H_\beta} & 0\\ 0 & 0 & 0\end{bmatrix} \quad \boldsymbol{D}_{en}=\begin{bmatrix}0 & 0 & 0\\ 0 & 0 & 0\\ 0 & 0 & \partial_z\end{bmatrix} \boldsymbol{A}_p=\begin{bmatrix}0 & 0 & \frac{1}{H_\alpha R_\alpha}\\ 0 & 0 & \frac{1}{H_\beta R_\beta}\\ 0 & 0 & 0\end{bmatrix} \boldsymbol{A}_n=\begin{bmatrix}\frac{1}{H_\alpha R_\alpha} & 0 & 0\\ 0 & \frac{1}{H_\beta R_\beta} & 0\\ 0 & 0 & 0\end{bmatrix} \tag{17}$$

Secondary variables are instead written and computed via constitutive physical relations:

$$\begin{aligned}
\boldsymbol{\sigma}_p &= \boldsymbol{C}^{\mathcal{E}}_{pp}\boldsymbol{\epsilon}_p + \boldsymbol{C}^{\mathcal{E}}_{pn}\boldsymbol{\epsilon}_n - \boldsymbol{e}^T_{pp}\boldsymbol{\mathcal{E}}_p - \boldsymbol{e}^T_{np}\boldsymbol{\mathcal{E}}_n\\
\boldsymbol{\sigma}_n &= \boldsymbol{C}^{\mathcal{E}}_{np}\boldsymbol{\epsilon}_p + \boldsymbol{C}^{\mathcal{E}}_{nn}\boldsymbol{\epsilon}_n - \boldsymbol{e}^T_{pn}\boldsymbol{\mathcal{E}}_p - \boldsymbol{e}^T_{nn}\boldsymbol{\mathcal{E}}_n\\
\boldsymbol{\mathcal{D}}_p &= \boldsymbol{e}_{pp}\boldsymbol{\epsilon}_p + \boldsymbol{e}_{pn}\boldsymbol{\epsilon}_n + \boldsymbol{\varepsilon}^{\epsilon}_{pp}\boldsymbol{\mathcal{E}}_p + \boldsymbol{\varepsilon}^{\epsilon}_{pn}\boldsymbol{\mathcal{E}}_n\\
\boldsymbol{\mathcal{D}}_n &= \boldsymbol{e}_{np}\boldsymbol{\epsilon}_p + \boldsymbol{e}_{nn}\boldsymbol{\epsilon}_n + \boldsymbol{\varepsilon}^{\epsilon}_{np}\boldsymbol{\mathcal{E}}_p + \boldsymbol{\varepsilon}^{\epsilon}_{nn}\boldsymbol{\mathcal{E}}_n
\end{aligned} \tag{18}$$

Reissner Mixed Variational Theorem is a mixed variational statement which permits to fulfil a priori the C^0_z-requirements for transverse shear and normal stresses and normal electric displacement. It can be used in various forms, among which:

$$\mathrm{R}MVT(u,\phi,\sigma_n): \int_V (\delta\boldsymbol{\epsilon}^T_{pG}\boldsymbol{\sigma}_{pC} + \delta\boldsymbol{\epsilon}^T_{nG}\boldsymbol{\sigma}_{nM} + \delta\boldsymbol{\sigma}^T_{nM}(\boldsymbol{\epsilon}_{nG}-\boldsymbol{\epsilon}_{nC}))dV = \delta L_e - \delta L^{in} \tag{19}$$

in which only the trasverse stresses are modelled.

A second form in which the normal electric displacement $\boldsymbol{\mathcal{D}}_z$ is primary variable in place of $\boldsymbol{\sigma}_n$:

$$\begin{aligned}
\mathrm{R}MVT(u,\phi,\mathcal{D}_z): \int_V (&\delta\boldsymbol{\epsilon}^T_{pG}\boldsymbol{\sigma}_{pC} + \delta\boldsymbol{\epsilon}^T_{nG}\boldsymbol{\sigma}_{nM} - \delta\boldsymbol{\mathcal{E}}^T_{pG}\boldsymbol{\mathcal{D}}_{pC} - \delta\boldsymbol{\mathcal{E}}^T_{nG}\boldsymbol{\mathcal{D}}_{nM} -\\
&\delta\boldsymbol{D}^T_{nM}(\boldsymbol{\mathcal{E}}_{nG}-\boldsymbol{\mathcal{E}}_{nC}))dV = \delta L_e - \delta L^{in}
\end{aligned} \tag{20}$$

A full form where both transverse stresses and normal electric displacement are enforced to be continuous at each layer interface:

$$\begin{aligned}
\mathrm{R}MVT(u,\phi,\sigma_n,\mathcal{D}_z): \int_V (&\delta\boldsymbol{\epsilon}^T_{pG}\boldsymbol{\sigma}_{pC} + \delta\boldsymbol{\epsilon}^T_{nG}\boldsymbol{\sigma}_{nM} - \delta\boldsymbol{\mathcal{E}}^T_{pG}\boldsymbol{\mathcal{D}}_{pC} - \delta\boldsymbol{\mathcal{E}}^T_{nG}\boldsymbol{\mathcal{D}}_{nM} +\\
&\delta\boldsymbol{\sigma}^T_{nM}(\boldsymbol{\epsilon}_{nG}-\boldsymbol{\epsilon}_{nC}) - \delta\boldsymbol{\mathcal{D}}^T_{nM}(\boldsymbol{\mathcal{E}}_{nG}-\boldsymbol{\mathcal{E}}_{nC}))dV = \delta L_e - \delta L^{in}
\end{aligned} \tag{21}$$

In these cases the constitutive equations for PVD (Eq.(18)) can be rearranged depending on the primary variables considered.

5 *FREE-VIBRATION OF PIEZOELECTRIC PLATES BY PVD MODELS*

Carrera Unified formulation was first applied to piezoelectric plates in [4] in the case of PVD. Results are summarized in Table 2-6.

In the Problem I a square plate with the side length a and the thickness h is considered. It consists of five layers which are assumed to be perfectly bonded to each other. The top and bottom layers are made of piezoelectric materials with the thickness $h^k_p = 0.1h$ each, the three structural layers of equal thickness have the configuration $[0°/90°/0°]$. The materials are PZT-4 for the piezoelectric and Gr/Ep for the structural layers. The corresponding material properties can be taken from Table 1. The top and bottom surfaces are assumed to be traction-free and electrically grounded,

Table 1: Elastic, piezoelectric and dielectric properties of used materials

Property	PZT-4	Gr/EP
E_1 [GPa]	81.3	132.38
E_2 [GPa]	81.3	10.756
E_3 [GPa]	64.5	10.756
ν_{12} [-]	0.329	0.24
ν_{13} [-]	0.432	0.24
ν_{23} [-]	0.432	0.49
G_{44} [GPa]	25.6	3.606
G_{55} [GPa]	25.6	5.6537
G_{66} [GPa]	30.6	5.6537
e_{15} [C/m^2]	12.72	0
e_{24} [C/m^2]	12.72	0
e_{31} [C/m^2]	-5.20	0
e_{32} [C/m^2]	-5.20	0
e_{33} [C/m^2]	15.08	0
$\tilde{\epsilon}_{11}/\epsilon_0$ [-]	1475	3.5
$\tilde{\epsilon}_{22}/\epsilon_0$ [-]	1475	3.0
$\tilde{\epsilon}_{33}/\epsilon_0$ [-]	1300	3.0

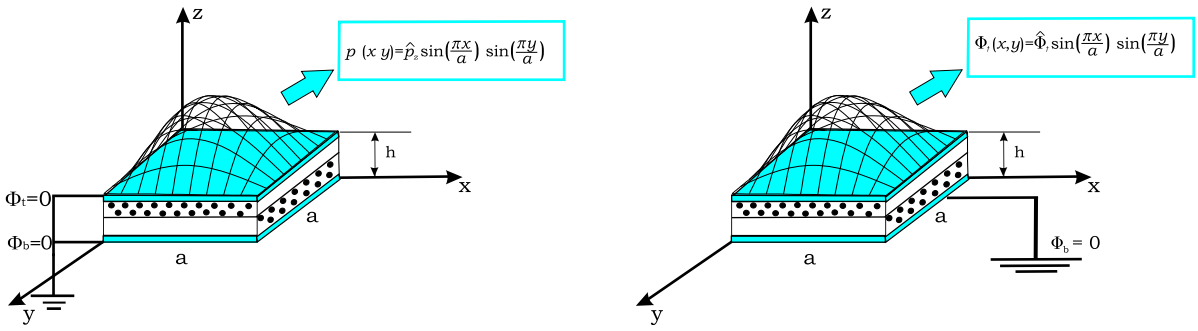

Figure 3: Considered multilayered piezoelectric plates: sensor configuration (left) and actuator configuration (right).

Table 2: Verification - Problem I, Frequency parameters $\gamma = \omega/100$ of exact solution and LD4

a/h		Mode 1	Mode 2	Mode 3	Mode 4	Mode 5	Mode 6
4	exact	57074.5	191301	250769	274941	362492	381036
	LD4	57074.0	191301	250768	274940	362489	381036
50	exact	618.118	15681.6	21492.8	209704	210522	378104
	LD4	618.104	15681.6	21492.6	209704	210522	378104

which imposes the electric potential to be zero ($\Phi_t = \Phi_b = 0$). The free vibration frequencies for one wave in each direction ($m = n = 1$) are calculated in means of the frequency parameter $\gamma = \omega/100$. Four thickness ratios $a/h = 2$, 4, 10 and 50 are considered. A 3D exact solution is available from Heyliger and Saravanos [14] for the cases $a/h = 4$ and 50. Further numerical results for these cases can be taken from Benjeddou [15] and Touratier and Ossadzow-David [16].

The configuration for Problem II consists of a simply supported square plate with the side length a and the thickness h. It is build of four layers, two layers of fiber reinforced material as a structural core on top and bottom of which the two piezoelectric layers are bonded. The core layers have the thickness $h_c = 0.4h$ each and the fiber direction is in $[0°/90°]$ configuration. The thickness of each piezoelectric layer is $h_p = 0.1h$. The materials are PZT-4 and Gr/Ep with the same properties as used for Problem I (Table 1). The analytic solution is calculated for one wave in each direction ($m = n = 1$). Four different thickness ratios $a/h = 2$, 4, 10 and 100 are considered in Table 6. A mechanical loading of $\hat{p}_z = 1$ is applied on the top surface of the plate. The top and bottom surfaces are electrically grounded and thus have the potential $\Phi_t = \Phi_b = 0$. The configuration of Problem II is the same of Problem I (Fig.3). 3D exact solution to Problems II for $a/h = 4$ were presented by Heyliger [17].

5.1 *VERIFICATION*

To verify CUF based models and to assess their accuracy a comparison with results from the 3D exact solution is presented. Attention is restricted to the LD4 plate theory which is supposed to lead to the best description (see also next section). The exact solution for Problem I taken is available for the thickness rations $a/h = 4$ and 50. Table 2 shows the results for the frequency parameter $\gamma = \omega/100$ for the first six modes of the exact solution and LD4 model of the Unified Formulation. The differences between the two solutions is extremely small. It can be concluded, that LD4 leads to a quasi-3D description of the dynamic and static response of multilayered plates embedding piezoelectric layers. LD4 therefore could be used as reference solutions in those cases in which 3D solutions are not available.

5.2 *ASSESSMENT OF VARIOUS MODELS*

Table 3 shows an overview of the frequency parameter results for all the considered theories for the thickness ratios $a/h = 4$ and 50. The results from the exact solution and the additional models of Benjeddou [18] and of Touratier and Ossadzow-David [16] are also listed. As expected the LDN models yield the best results. The ESL models with imposed zig-zag form EDZN lead in the most cases to a slight improvement compared to the EDN models.

5.2.1 *INFLUENCE OF ORDER OF EXPANSION*

In Table 4 the influence of the order of expansion N on the first mode of LDN and EDN models is summarized. For each model the number of degrees of freedom (NDOF) and the error to the exact solution (LD4) is given. For the LDN models an increase from $N = 1$ to 4 has nearly no effect, because even LD1 yields only marginal errors. For the ED models in contrast, N is more relevant. The thick plate case requires at least third order and the thin plate case at least quadratic expansion to obtain good results. Comparing the higher order EDN with the lower order LDN models it can be noted, that for the given problem the latter yield better results although the implied NDOF is nearly the same.

Table 3: Problem I, Frequency parameters $\gamma = \omega/100$ for $a/h = 4$ and $a/h = 50$

	$a/h = 4$			$a/h = 50$		
	Mode 1	Mode 2	Mode 3	Mode 1	Mode 2	Mode 3
exact	57074.5	191301	250769	618.118	15681.6	21492.8
Touratier	-	194903	251763	-	15592.3	-
Benjeddou	58216.1	196018	268650	618.435	15684.0	21499.4
LD4	57074.0	191301	250768	618.104	15681.6	21492.6
LD1	57252.5	194840	255646	619.022	15683.4	21499.4
ED4	58713.8	194592	254740	618.464	15693.5	21497.8
ED1	74105.9	196021	266337	689.867	15695.0	21507.4
EDZ3	57656.7	195711	259570	618.382	15687.1	21496.5
EDZ1	63204.7	195965	266196	688.082	15693.6	21498.5
FSDT	74106.0	198465	286795	689.867	15877.2	22943.9
CLT	102932	198465	286795	719.427	15877.2	22943.9

Table 4: Problem I, Influence of Order of Expansion N on first frequency parameter γ of LDN- and EDN-models

		LDN			EDN		
a/h	N	NDOF	γ_1	Δ[%]	NDOF	γ_1	Δ[%]
4	4	84	57074.0		36	58713.8	2.87
	3	64	57074.0	0.000	28	58818.6	3.06
	2	44	57081.9	0.014	20	69413.7	21.6
	1	24	57252.5	0.313	12	74105.9	29.84
50	4	84	618.104		36	618.464	0.06
	3	64	618.104	0.000	28	618.550	0.07
	2	44	618.105	0.000	20	620.229	0.34
	1	24	619.022	0.149	12	689.867	11.61

Table 5: Problem I, Influence of piezoelectric effect on first frequency parameters γ_1

$a/h =$	2	4	10	50
LD4	136604	57074.0	13526.4	618.104
LD4m	136598	57063.6	13520.7	617.770
Δ[%]	0.004	0.018	0.042	0.054

Table 6: Problem II, Selected results for w, σ_{xx}, σ_{xz}, Φ and $\tilde{D}_z$

$a/h =$		2	4	10	100
	LD4	4.9113	30.029	582.06	4675300
	LD1	4.8087	29.852	579.26	4647300
$w \times 10^{11}$	ED4	4.5047	28.591	573.25	4673900
at	ED1	2.8575	18.488	423.29	3668700
$z = 0$	EDZ1	2.9117	20.153	498.04	4435100
	FSDT	2.8575	18.488	423.29	3668700
	CLT	0.58607	9.3884	364.43	2593400
	LD4	3.2207	6.5642	32.771	3142.1
	LD1	3.5181	6.9995	34.256	3266.9
σ_{xz}					
at	LD4	0.26995	0.68720	1.8540	18.832
$z = 0$					
	LD4	0.9103	6.1084	44.471	4580.2
	LD1	0.8597	6.0303	44.175	4552.7
$\Phi \times 10^3$	ED4	0.94157	6.1274	44.402	4568.9
at	ED1	0.78657	2.6580	15.044	1470.3
$z = 0$	EDZ1	1.3901	6.3499	41.379	4171.8
	FSDT	0.78657	2.6580	15.044	1470.3
	CLT	0.38494	2.1095	14.366	1040.5
	LD4	0.0256	0.0161	0.0139	0.0136
	LD1	-0.0662	-0.0880	-0.2853	-23.838
$\tilde{D}_z \times 10^9$	ED4	0.0489	0.0353	0.0327	0.0324
at	ED1	0.0834	0.0464	-0.1163	-18.729
$z = h/2$	EDZ1	0.1496	0.1397	0.1372	0.1367
	FSDT	0.0615	0.0401	-0.1174	-18.729
	CLT	-0.0088	-0.0314	-0.1883	-13.311

5.2.2 *INFLUENCE OF PIEZOELECTRIC EFFECT*

The influence of the piezoelectric coupling effects on the free vibration of the considered plate is examined in Table 5. The results are calculated with the presented LD4 model, for the mechanical case neglecting the piezoelectric coupling terms and thus considering only the elastic properties of the piezoelectric layers (LD4m). The coupling effect can be interpreted as an additional stiffness of the plate, but at least in the considered problem this influence on the natural frequencies is negligible.

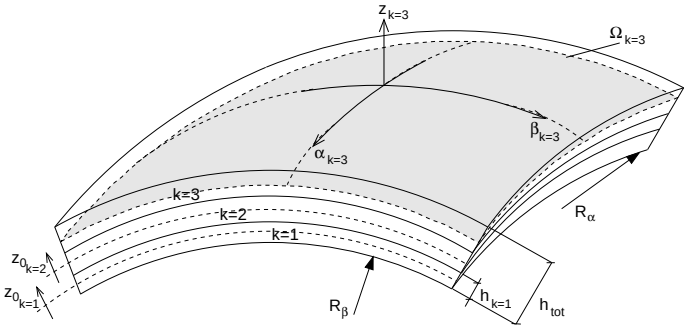

Figure 4: Notations for the description of the shell geometry.

6 *FREE-VIBRATION OF PIEZOELECTRIC SHELLS BY PVD MODELS*

Extension of CUF to PVD piezoelectric shells was given in [19] and [20]. A discussion of the main point is herein given. For the free-vibration problem of multilayered, piezoelectric shells only few works are available in open literature presenting exact 3D-solutions. Verification computations are presented considering the results obtained by Drumheller and Kalnins in [21] for an homogeneous piezoelectric cylinder and those obtained by Heyliger et al. in [22] for a laminated ring. Finally, the eigenfrequencies of a laminated cylinder are presented and the effects of the electro-mechanical coupling are discussed.

Drumheller and Kalnins [21] analyze the free-vibration response of a simply-supported cylinder constituted by homogeneous piezoelectric material with short-circuited surfaces. Cylinders of variable length a are considered; the mean line radius is $R_\beta = 11.1125$ mm and the shell thickness is $h = 3.175$ mm (the material data are reported in Tab. 7). The two considered vibration modes are schematically represented in Fig. 5. These modes are obtained in the present theory by setting $m = 1$ (fundamental mode in the cylinder axis) and $n = 0$ (axisymmetric mode, i.e. $\beta = 0$).

Table 7: Material data for the piezoelectric cylinder of Ref. [21].

material constants for PZT-4					
$C^E_{11} = C^E_{22}$	139.89	GPa	$e_{31} = e_{32}$	-5.5864	C/m^2
C^E_{33}	113.16	GPa	e_{33}	16.3801	C/m^2
C^E_{12}	78.62	GPa	$e_{15} = e_{24}$	12.2013	C/m^2
$C^E_{13} = C^E_{23}$	76.54	GPa	$\varepsilon^S_{11} = \varepsilon^S_{22}$	$59.77\ 10^{-10}$	C/Vm
$C^E_{44} = C^E_{55}$	26.91	GPa	ε^S_{33}	$58.57\ 10^{-10}$	C/Vm
C^E_{66}	30.64	GPa	ρ	$7.5\ 10^3$	kg/m^3

Heyliger et al. give in [22] the natural frequencies of a laminated ring consisting of an inner isotropic, elastic layer of Titanium (Ti) and an outer piezoceramic layer (PZT-4). The geometry

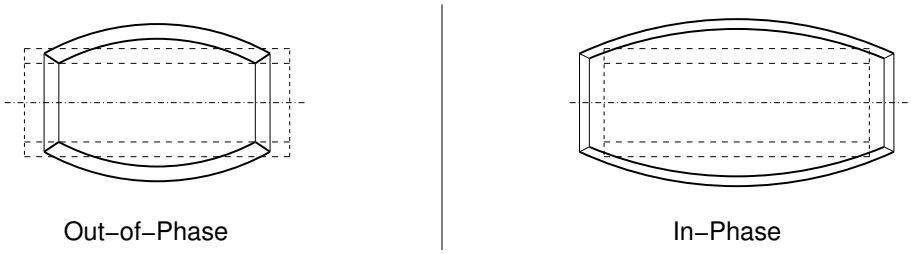

Figure 5: Axisymmetric modes of a piezoelectric cylinder considered in Ref. [21]

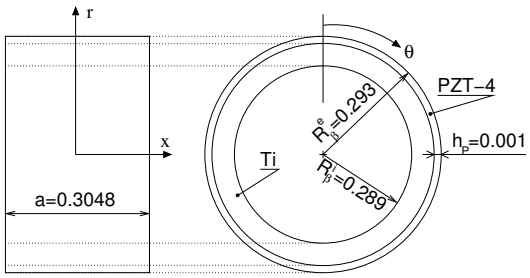

$E_1 = 81.3$ GPa	$e_{15} = 12.72$ C/m^2
$E_3 = 64.5$ GPa	$e_{31} = -5.20$ C/m^2
$\nu_{13} = 0.432$	$e_{33} = 15.08$ C/m^2
$\nu_{12} = 0.329$	$\varepsilon_{11} = 1475\,\varepsilon_0$
$G_{44} = 25.6$ GPa	$\varepsilon_{33} = 1300\,\varepsilon_0$
$\rho = 7600$ kg/m^3	$\varepsilon_0 = 8.85\,10^{-12}$ C/Vm

Figure 6: Left: Geometry of the laminated ring considered in Ref. [22] (all quantities given in [m]). Right: Data for transversally isotropic PZT-4 material

Table 8: Natural frequencies [Hz] for the layered ring presented in Ref. [22]. The values in parentheses are the relative percentual difference with respect to the reference solution.

	$n = 4$	$n = 8$	$n = 12$	$n = 16$	$n = 20$
Ref. [22]	31.27	170.42	407.29	745.21	1190.48
LD4	31.64 (1.18)	171.60 (0.69)	406.87 (0.10)	736.08 (1.23)	1158.53 (2.68)
LD1	33.28 (6.43)	180.51 (5.92)	427.99 (5.08)	774.25 (3.90)	1218.56 (2.36)
ED4	31.65 (1.22)	171.64 (0.72)	406.98 (0.08)	736.28 (1.20)	1158.87 (2.66)
ED1	35.54 (13.66)	192.74 (13.10)	456.95 (12.19)	826.54 (10.91)	1300.67 (9.26)

of the ring is depicted in Fig. 6 (left), where the coordinates and notations defined in Fig. 4 have been employed. To reduce the computational cost, only a quarter of the ring has been considered in Ref. [22], and various symmetry conditions holding on the edges $\theta = 0$, $\theta = \pi/2$ and $x = 0$ (see Fig. 6) are given as boundary conditions for the dynamic analysis. The piezoelectric layer is polarized in radial direction and has a thickness of $h_P = 0.25h = 0.001$ m. The employed material parameters for the titanium layer are $E = 114$ GPa, $\nu = 0.3$, $\rho = 2768$ kg/m^3 and $\varepsilon = \varepsilon_0 = 8.85\ 10^{-12}$ C/Vm; those for PZT-4 are given in Fig. 6 (right). In Ref. [22], a Finite Element (FE) formulation is presented based on a layerwise description of the coupled electro-mechanical problem. The symmetry conditions corresponding to a vanishing circumferential displacement on the edges $\theta = 0$ and $\theta = \pi/2$ as well as to a vanishing axial displacement at $x = 0$ (group 7 of the cited reference) are represented within the present formulation by $m = 0$ and $n = 4, 8, 12, 16, 20$. Only the mode characterized by a pure circumferential deformation has been considered, i.e. $\hat{u}^k_{\alpha\tau} = 0$. The electrical boundary conditions consist of a short-circuit between the top and bottom surface of the piezoelectric layer. Tab. 8 reports the results obtained by the present formulations as well as the relative difference (in percent) with respect to the values of Ref. [22]. It can be seen that a qualitative jump is associated to the consideration of the electrical stiffness introduced by an at least quadratic assumption for the electric potential: in fact, all linear formulations (LD1, ED1) provide results of clearly lower quality, the relative models resulting always too stiff. Except for slight differences in the higher modes, the closed-form solutions of all formulations present a good agreement with the approximate FE solution proposed in literature. It is interesting to note that, for higher modes, the analytical solution for less accurate formulations represents better the FE solution. This may be due to the superimposition of two distinct errors, i.e. the discretization error and the error in the thickness assumptions, which cancel out, thus providing a better agreement.

7 *FE ANALYSIS BY RMVT AND PVD STATEMENTS*

PVD results are in this section compared to RMVT(u, ϕ, σ_n) ones. Results are restricted to plate geometries. A few results are taken by the quite exhaustive archivial articles [**?**]. The exact solution for a hybrid laminate containing both piezoelectric and elastic layers under applied surface traction (*direct effect*) and applied electric potential (*converse effect*) has been presented by Heyliger [14] and will be herein used as a benchmark for our finite element models, even if only results for a thick plate (S=4) are given.

The results are presented for a simply supported cross-ply laminate $[0°/90°]$ composed of an elastic material with piezoelectric layers bonded to the upper and lower surfaces. The plate has side lengths $a = b$ and a total thickness h. The elastic layers have thickness of $0.4h$ and the thickness of the piezoelectric layers is $0.1h$. The material data are listed in Tab.(1). Only the electric potential is compared in the case of actuators and sensors layers. In the sensor problem the electric boundary condition are those of a short-circuited plate. From the obtained results the following main remarks can be pointed out:

- All the results are very close to those obtained by the closed-form solution.
- The first order models ED1 and EM1 lead to inaccurate results especially for thick plates. At the same time these models are very sensible to the introduction of the Murakami's function. See Tab.(9).
- Slight differences are appreciable in the changing of the variational principle for displacements and electric fields but the use of the RMVT is fundamental in first order models for the modelization of normal stress.

- Second order models are at least required to describe the through-thickness profile of the electric potential for ESL models: see Tab.(9). On the contrary, first order LW models match very well the exact solution.
- The use of the mixed variational principle improves the results of the electric potential especially for lower order models. See Tab.(9)
- In general the actuator model could show some difficulties in matching the top and bottom surface values.

Table 9: Piezoelastic analysis - sensor and actuator configurations: Electric potential $\phi(\frac{a}{2}, \frac{b}{2}, 0)$ results.

Piezoelastic analysis - sensor configuration $\phi(\frac{a}{2}, \frac{b}{2}, 0)$ Q9 $[6 \times 6]$				
S	**4**	**10**	**20**	**100**
Exact[14]	$6.11E-3$	–	–	–
LD 1	$6.0111E-3$	$4.4392E-2$	$1.8349E-1$	4.6512
LM 1	$6.0388E-3$	$4.4781E-2$	$1.8469E-1$	4.6689
LD 4	$6.1176E-3$	$4.4776E-2$	$1.8463E-1$	4.6770
LM 4	$6.1180E-3$	$4.4786E-2$	$1.8464E-1$	4.6770
ED 1	$2.6635E-3$	$1.5154E-2$	$6.0010E-2$	1.5016
EM 1	$3.2110E-3$	$2.0136E-2$	$8.1124E-2$	2.0401
ED 4	$6.1351E-3$	$4.4705E-2$	$1.8425E-1$	4.6676
EM 4	$6.1442E-3$	$4.4735E-2$	$1.8427E-1$	4.6667
EDZ1	$6.1365E-3$	$4.1434E-2$	$1.6882E-1$	4.2611
EMZ1	$6.1073E-3$	$4.1508E-2$	$1.6927E-1$	4.2733
EDZ3	$6.3462E-3$	$4.5007E-2$	$1.8481E-1$	4.6764
EMZ3	$6.3326E-3$	$4.5000E-2$	$1.8478E-1$	4.6748
Piezoelastic analysis - actuator configuration $\phi(\frac{a}{2}, \frac{b}{2}, 0)$ Q9 $[6 \times 6]$				
S	**4**	**10**	**20**	**100**
Exact[14]	$4.476E-1$	–	–	–
LD 1	$4.4693E-1$	$4.9788E-1$	$4.9101E-1$	$4.9992E-1$
LM 1	$4.4698E-1$	$4.9788E-1$	$4.9101E-1$	$4.9992E-1$
LD 3	$4.4801E-1$	$4.9785E-1$	$4.9103E-1$	$4.9992E-1$
LM 3	$4.4801E-1$	$4.9785E-1$	$4.9102E-1$	$4.9992E-1$
LD 4	$4.4801E-1$	$4.9785E-1$	$4.9103E-1$	$4.9992E-1$
LM 4	$4.4801E-1$	$4.9785E-1$	$4.9102E-1$	$4.9992E-1$
ED 1	$4.4621E-1$	$4.9784E-1$	$4.9088E-1$	$4.9992E-1$
EM 1	$4.4614E-1$	$4.9783E-1$	$4.9087E-1$	$4.9992E-1$
ED 4	$4.4844E-1$	$4.9787E-1$	$4.9110E-1$	$4.9992E-1$
EM 4	$4.4840E-1$	$4.9787E-1$	$4.9109E-1$	$4.9992E-1$
EDZ1	$4.4816E-1$	$4.9785E-1$	$4.9104E-1$	$4.9992E-1$
EMZ1	$4.4807E-1$	$4.9785E-1$	$4.9102E-1$	$4.9992E-1$
EDZ3	$4.4842E-1$	$4.9787E-1$	$4.9110E-1$	$4.9992E-1$
EMZ3	$4.4839E-1$	$4.9787E-1$	$4.9109E-1$	$4.9992E-1$

8 *FE ANALYSIS BY RMVT WITH A PRIORI EVALUATION OF ELECTRICAL DISPLACEMENT*

This section shows the performances of the FEs based on RMVT$(u, \phi, \sigma_n, \mathcal{D}_z)$ for static response (sensor configuration). Results are taken by [6] and [7]. Results for the plate problem already considered in the previous analysis are given in Tab.10; here a comparison between the RMVT$(u, \phi, \sigma_n, \mathcal{D}_z)$ and the RMVT$(u, \phi, \mathcal{D}_z)$ statements for different thickness ratios and different FEs is made. It has been showed results concerning a $Q4$ element because is the best solution in terms of adequacy of the responses and time required. What deserves to be mentioned is the importance of the UF where the order of the expansion N is taken as a free parameter and in this case a better solution is obtained when a higher order of expansion is considered. The RMVT$(u, \phi, \sigma_n, \mathcal{D}_z)$ is also suitable for the electric potential. In fact, in order to obtain the exact profile in the-through-the-thickness direction, a second order LW-FE is required with the RMVT$(u, \phi, \mathcal{D}_z)$ whereas the same response is obtained with a first order by means of the RMVT$(u, \phi, \sigma_n, \mathcal{D}_z)$: as a consequence the same appropriate response is obtained with the third part of the time required by the RMVT$(u, \phi, \mathcal{D}_z)$.

Table 10: $D_z \times 10^{13}$ for $(\frac{a}{2}, \frac{b}{2}, 0.5)$, mesh$[12 \times 12]$ and Q4 elements.

$\frac{a}{h}$	2	4	10
exact 3D [17]	/	160.58	/
LM4	261.73	161.50	137.55
LM4*	316.30	301.4	941.94
LD4	284.94	212.66	439.78
LM3	263.79	161.89	137.70
LM3*	306.17	299.41	942.06
LD3	286.90	213.17	417.54
LM2	254.67	153.87	130.17
LM2*	310.83	290.39	923.49
LD2	300.96	223.83	430.72
EMZ3	549.81	371.98	350.39
EM4	516.85	357.11	346.49
EM3	608.59	283.71	235.48

Shell geometries were discussed in [6]. Results in Tab.11 confirm the conclusions made for plates geometries.

9 *FE ANALYSIS BY RMVT-D_z*

A quite interesting application of Reissner ideas is obtained by only considering interlaminar continuity of normal electric displacement $\mathcal{D}_z$. No additional degrees of freedom are introduced by transverse shear stresses. Evaluation of normal electrical displacement is very much improved with respect to PVD evaluation. Such accurate evaluation permits a priori calculation of electrical charge which plays a fundamental role in practical applications of smart structures. Results are given in Tabs.12-13 and Figure 7.

10 *ACKNOWLEDGEMENTS*

First authors acknowledge the contribution of co-workers D Ballahuse, M D'Ottavio, M Boscolo, C Fagiano, A Robaldo and P Nali.

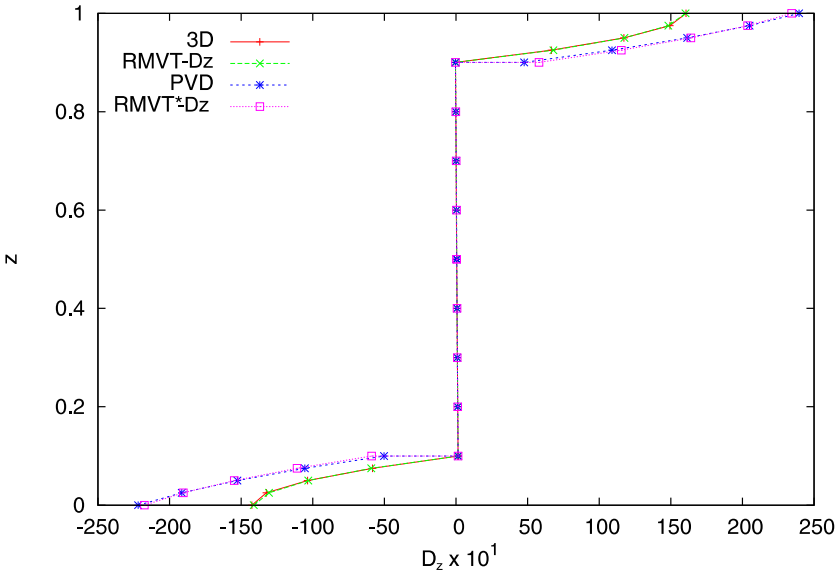

Figure 7: Comparison between FEM and 3D-exact solutions, sensor case; the electric displacement is in $[c/m^2]$; $D_z = D_z(a/2, b/2)$; the D_z RMVT-D_z* is calculated by constitutive relations in the RMVT-D_z analysis

References

[1] Chopra I, 2002, *Review of State of Art of Smart Structures and Integrated Systems*, AIAA Journal, vol. 40, pp. 2145–2187.

[2] Carrera E, 1997, *An improved Reissner-Mindlin-Type model for the electromechanical analysis of multilayered plates including piezo-layers.* Journal of Intell. Mat. Syst. and Stru., vol. 8, pp. 232-248.

[3] Gopinathan SV, Varadan VV, Varadan VK, 2000, *A review and critique of theories for piezoelectric laminates*, Smart Materials and Structures, vol. 9, pp. 24-48.

[4] Ballhause S, D'Ottavio M, Kröplin B, Carrera E, 2004, *A Unified Formulation to Assess Multilayered Theories for Piezoelectric Plates.* Computers & Struc., vol. 83, pp. 1217-1235.

[5] Carrera E, Boscolo M, 2007, *Classical and Mixed elements for static and dynamic analysis of piezoelectric plates.* Int. Journal for Num. Meth in Eng., vol. 70, pp. 253-291.

[6] Carrera E, Brischetto S, 2007, *Piezoelectric Shells Theories with 'a priori' Continuous Transverse Electro-Mechanical Variables.* Journal of Mech. of Mat. and Struc., vol. 2, pp. 377-398.

[7] Carrera E, Fagiano C, 2007, *Mixed piezoelectric plate elements with continuous transverse electric displacements.* Journal of Mech. of Mater. and Struct., vol. 2, pp. 421-438.

[8] Carrera E, Brischetto S, 2007, *Reissner Mixed Theorem Applied to Static Analysis of Piezoelectric Shells.* Journal of Intell. Mat. Syst. and Stru., vol. 18, pp. 1083-1107.

[9] Carrera E, Brischetto S, Nali P, 2008, *Variational Statements and Computational Models for Multifield Problems and Multilayered Structures.* Mech. Adv. Mater. Struct., vol. 15, pp. 182-198.

[10] Carrera E, Nali P, 2009 *A comprehensive FE model for the analysis of Multilayered Structures Subjected to Multifled Loadings.* International Journal of Solids and Structures, in press

[11] Carrera E, 1995, *A class of two-dimensional theories for anisotropic multilayered plates analysis.* Atti della Accademia delle Scienze di Torino. Classe di scienze fisiche matematiche e naturali, vol. 19-20, pp. 1-39.

[12] Carrera E, 1998, *Evaluation of layer-wise mixed theories for laminated plates analysis.* AIAA Journal, vol. 36, pp. 830–839.

[13] Murakami H, 1986, *Laminated composite plate theory with improved in-plane response.* Journal of Applied Mechanics, vol. 53, pp. 661-666.

[14] Heyliger P and Saravanos D A, 1995, *Exact free-vibration analysis of laminated plates with embeded piezoelectric layers.* Journal of the Acoustical Society of America, vol.98(3), pp. 1547-1557.

[15] Benjeddou A, 2000, *Advanced in piezoelectric finite element modeling of adaptive structural elements: a survey.* Computers and Structures, vol.76, pp. 347-363.

[16] Touratier M and Ossadzow-David C, 2003, *Multilayered piezoelectric refined plate theory.* AIAA Journal, vol. 41(1), pp. 90–99.

[17] Heyliger P, 1994, *Static behavior of laminated elastic/piezoelectric plates.* AIAA Journal, vol. 32(12), pp. 2481–2484.

[18] Benjeddou A and Deü J-F, 2001, *A two-dimensional closed-form solution for the free-vibrations analysis of piezoelectric sandwich plates.* International Journal of Solids and Structures, vol. 39, pp. 1463–1486.

[19] Carrera E, 1999, *A study of transverse normal stress effect on vibration of multilayered plates and shells.* Journal of Sound and Vibrations, vol. 225 (5), pp. 803–829.

[20] D'Ottavio M, Ballhause D, Kroplin B, Carrera E, 2006, *Closed form solutions for the free vibration problem of multilayered piezoelectric shells.* Computers and Structures, vol. 84, pp. 1506-1518.

[21] Drumheller D S, Kalnins A, 1957, *Dynamic shell theory for ferroelectric ceramics.* Journal of Acoustical Society of America, vol. 47, pp. 1343–1353.

[22] Heyliger P, Pei K C, Saravanos D A, 1996, *Layerwise mechanics and finite element model for laminated piezoelectric shells.* AIAA Journal, vol. 34 (11), pp. 2353–2360.

[23] Carrera E, Boscolo M, Robaldo A, 2007, *Hierarchic multilayered plate elements for coupled multifiled problems of piezoelectric adaptive structures: formulation and numerical assessment.* Archives of Computational Methods in Engineering, vol. 14, pp.383-430.

Table 11: Proposed benchmark: one piezoelectric layer for the Varadan and Bhaskar cylindrical shell. Comparison of various approaches. Actuator case.

R_β/h	2	4	10	100
		Φ a $z=0$		
$LD4$	0.3431	0.4611	0.5037	0.5254
$LM1$	0.5000	0.5000	0.5000	0.5000
$LM4$	0.3431	0.4611	0.5037	0.5254
$LFM1$	0.5000	0.5000	0.5000	0.5000
$LFM4$	0.3431	0.4611	0.5037	0.5254
		$\mathcal{D}_z 10^{11}$ a $z=h/2$		
$LD4$	-605.73	-801.76	-1622.9	-10416
$LM1$	-350.00	-662.37	-1608.6	-11711
$LM4$	-605.73	-801.76	-1622.9	-10416
$LFM1$	-327.37	-642.20	-1599.7	-16656
$LFM4$	-584.80	-783.99	-1615.6	-16266
		$W10^{11}$ a $z=0$		
$LD4$	-9.6220	-11.285	6.4540	11277
$LM1$	-21.851	-18.528	2.9362	9531.4
$LM4$	-9.6220	-11.285	6.4540	11277
$LFM1$	-21.850	-18.528	2.9353	9531.4
$LFM4$	-9.6220	-11.285	6.4540	11277
		σ_{zz} a $z=h/2$		
$LD4$	3.0350	2.5512	1.0498	-836.32
$LM1$	-0.4037	-0.1264	0.6259	54.231
$LM4$	0.0431	0.0114	0.0004	-0.0001
$LFM1$	-0.4037	-0.1264	0.6258	54.231
$LFM4$	0.0431	0.0114	0.0004	-0.0001

Table 12: Comparison between FEM and 3D-exact solutions, actuator case. LD2 and LM2 FEs are employed for PVD and RMVT case, respectively. The electric displacement is in $[c/m^2]$. $D_z = D_z(a/2, b/2)$. The D_z RMVT-$D_z{}^*$ is calculated by constitutive relations in the RMVT-D_z analysis.

	$D_z \times 10^{13}$		
Height	$RMVT$-D_z	PVD	$RMVT$-D_z^*
1.000	-2.4431	-2.4382	-2.4385
0.900	-4.1321	-4.1504	-4.0924
0.900	-4.1321	-4.1274	-4.1294
0.500	-3.1229	-3.1182	-3.1145
0.500	-3.1229	-3.1275	-3.1313
0.100	-2.8095	-2.8142	-2.8123
0.100	-2.8095	-2.8425	-2.8823
0.000	-2.7316	-2.7507	-2.7307

Table 13: Comparison between PVD and RMVT-D_z results, sensor case. LD2 or LM2 FEs are employed. Q is the charge at the top surface of the top layer and it is expressed in $[c]$. RMVT-D_z* result is computed starting from the D_z calculated by constitutive relations in the RMVT-D_z analysis.

$Qx10^{11}(RMVT - D_z)$	$Qx10^{11}(PVD)$	$Qx10^{11}(RMVT - D_z*)$
10.219	8.8763	8.5457